Geophysical Research Letters

RESEARCH LETTER
10.1029/2024GL110157

From the Surface to the Stratosphere: Large-Scale Atmospheric Response to Antarctic Meltwater

Rebecca L. Beadling[1], Pu Lin[2], John Krasting[3], William Ellinger[1], Anna Coomans[1], James Milward[1], Katherine Turner[2,3,4], Xiaoqi Xu[5,6,7], Torge Martin[7], and Maria J. Molina[8,9]

[1]Department of Earth and Environmental Science, Temple University, Philadelphia, PA, USA, [2]Princeton University Atmospheric and Oceanic Sciences Program, Princeton, NJ, USA, [3]NOAA, Geophysical Fluid Dynamics Laboratory, Princeton, NJ, USA, [4]Department of Geosciences, University of Arizona, Tucson, AZ, USA, [5]State Key Laboratory of Numerical Modelling for Atmospheric Sciences and Geophysical Fluid Dynamics, Institute of Atmospheric Physics, Chinese Academy of Sciences, Beijing, China, [6]University of Chinese Academy of Sciences, Beijing, China, [7]GEOMAR Helmholtz Centre for Ocean Research Kiel, Kiel, Germany, [8]Department of Atmospheric and Oceanic Science, University of Maryland, College Park, MD, USA, [9]National Science Foundation National Center for Atmospheric Research, Boulder, CO, USA

Abstract The ocean response to Antarctic Ice Sheet (AIS) mass loss has been extensively studied using numerical models, but less attention has been given to the atmosphere. We examine the global atmospheric response to AIS meltwater in an ensemble of experiments performed using two fully coupled climate models under a pre-industrial climate. In response to AIS meltwater, the experiments yield cooling from the surface to the tropopause over the subpolar Southern Ocean, warming in the Southern Hemisphere polar stratosphere, and cooling in the upper tropical troposphere. Positive feedbacks, initiated by disrupted ocean-atmosphere heat exchange, result in a change in the top-of-atmosphere radiative balance caused primarily through surface and near-surface albedo changes. Changes in the atmospheric thermal structure alter the jet streams aloft. The results highlight the global influence of AIS melting on the climate system and the potential for impacts on mid-latitude climate patterns and delayed regional warming signals.

Plain Language Summary The Antarctic Ice Sheet is expected to melt as the climate warms and many studies have focused on understanding how the ocean state might respond. How the structure of the global atmosphere, including temperature and global wind patterns, will respond to this added meltwater and associated ocean state changes remains unclear. We investigate changes in atmospheric properties including temperature, clouds, radiation, water vapor, and global wind patterns that occur when meltwater is added to the Antarctic coast in two climate models. We find temperatures within the troposphere to generally decrease, whereas temperatures in the stratosphere increase over the Southern Hemisphere polar region. Temperatures also decrease in the high-altitude troposphere near the equator. Changes throughout the atmosphere, including clouds and water vapor, in combination with changes in atmosphere-ocean heat exchange, impact the amount of energy within the climate system. Changes in the temperature structure of the atmosphere have far-reaching effects on global wind patterns. The response to isolated Antarctic Ice Sheet melting, which we present, generally opposes that found for typical global warming scenarios lacking the ice sheet response. All of this highlights the remote consequences of Antarctic Ice Sheet melting.

Key Points:

- Freshwater is added along the coast of Antarctica in two climate models and changes in the full-column global atmosphere are investigated
- Temperature changes extend from the surface to the stratosphere and from the Southern Ocean to the upper tropical troposphere
- Meltwater-induced changes in the atmosphere's thermal structure result in altered large-scale wind patterns

Supporting Information:

Supporting Information may be found in the online version of this article.

Correspondence to:

R. L. Beadling,
rebecca.beadling@temple.edu

Citation:

Beadling, R. L., Lin, P., Krasting, J., Ellinger, W., Coomans, A., Milward, J., et al. (2024). From the surface to the stratosphere: Large-scale atmospheric response to Antarctic meltwater. *Geophysical Research Letters*, *51*, e2024GL110157. https://doi.org/10.1029/2024GL110157

Received 20 MAY 2024
Accepted 19 OCT 2024

Author Contributions:

Conceptualization: Rebecca L. Beadling
Formal analysis: Rebecca L. Beadling, William Ellinger, Xiaoqi Xu
Investigation: Pu Lin, John Krasting, Katherine Turner, Xiaoqi Xu, Torge Martin, Maria J. Molina
Methodology: Rebecca L. Beadling
Visualization: Rebecca L. Beadling, William Ellinger, Anna Coomans
Writing – original draft: Rebecca L. Beadling
Writing – review & editing: Pu Lin, John Krasting, James Milward,

1. Introduction

Significant mass loss from the Antarctic Ice Sheet (AIS) has been observed in recent decades in response to global warming (Smith et al., 2020). AIS mass loss is concerning given its potential to raise global sea level (Fox-Kemper et al., 2021) and alter large-scale ocean and atmospheric circulation patterns which will directly impact humans and ecosystems. Despite its potential as an important climate forcing (Schmidt et al., 2023), AIS meltwater and potential feedbacks onto the global climate system have not been accounted for in historical simulations and climate projections due to the general lack of dynamic ice sheet components included in coupled climate models. Recognizing the need to constrain the climate response to AIS meltwater in order to reduce projection uncertainty, there is a rich history and growing number of studies which have prescribed additional freshwater anomalies in the Southern Ocean (SO) to document the ocean, sea ice, and climate response (Stouffer et al., 2007, Table 1 of Swart et al., 2023). Cooling of sea surface temperatures (SSTs), expansion of Southern Hemisphere (SH) sea ice, surface freshening, SO subsurface warming, and a reduction of Antarctic Bottom Water

Katherine Turner, Xiaoqi Xu, Torge Martin, Maria J. Molina

have emerged as robust simulated responses to AIS meltwater (Stouffer et al., 2007; comprehensive list in Table 1 of Swart et al., 2023). The ocean-sea ice response is a result of an anomalously fresh surface layer reducing the upward vertical mixing of subsurface heat and thereby reducing surface heat fluxes from the ocean to the atmosphere or sea ice (Chen et al., 2023; Stouffer et al., 2007). A fresh and cooler surface layer supports enhanced sea ice growth, further reducing surface temperatures.

Despite most published results from AIS meltwater perturbation studies utilizing a fully coupled atmosphere-ocean configuration (Swart et al., 2023), much less attention has been given to the large-scale atmospheric response. Analysis of the atmospheric response has mostly been limited to metrics at the surface or in the lower troposphere. Results suggest pronounced surface cooling or reduced transient warming (Bronselaer et al., 2018; Dong et al., 2022; Park & Latif, 2019), a northward shift of the Intertropical Convergence Zone (ITCZ; Stouffer et al., 2007; Ma & Wu, 2011; Bronselaer et al., 2018; Park & Latif, 2019; Dong et al., 2022), increased SO low-cloud cover (Dong et al., 2022), and an intensification of SH surface wind stress (Ma & Wu, 2011).

The strong surface cooling exhibited in AIS meltwater studies imply a redistribution of energy within the climate system. Such changes are likely to influence large-scale atmospheric circulation patterns, moisture content (Held & Soden, 2006), and cloud distribution (Dong et al., 2022), invoking a response beyond the planetary boundary layer which has yet to be fully explored in meltwater perturbation studies. Here we analyze the atmospheric response to AIS meltwater simulated in two coupled climate models, highlighting the global influence of AIS mass loss on the atmospheric structure.

2. Methods

2.1. Climate Models

The GFDL-CM4 fully coupled climate model and GFDL-ESM4 Earth System model developed at the Geophysical Fluid Dynamics Laboratory (GFDL) of the National Oceanic and Atmospheric Administration (NOAA) are used in this study. A comprehensive description of CM4 and ESM4 can be found in Adcroft et al. (2019), Held et al. (2019), Dunne, Bociu, et al. (2020), and Dunne, Horowitz et al. (2020). Beadling et al. (2022) and Tesdal et al. (2023) describe the ocean-sea ice response in the meltwater experiments studied here and provide details on the relevant differences between the two models, focusing on the ocean configurations. Both models use the GFDL-OM4.0 ocean/sea-ice model (Adcroft et al., 2019) based on MOM6 with a nominal horizontal grid spacing of 25 km in CM4 and 50 km in ESM4. The sea ice model within GFDL-OM4.0 is SIS2.0 with a horizontal grid spacing equivalent to that of the ocean.

The atmosphere in CM4 is the GFDL Atmospheric Model version 4.0 (AM4.0; Zhao et al., 2018a, 2018b) with 33 vertical levels extending to 100 Pa (~45 km) and a nominal 100 km horizontal grid spacing. AM4.0 is considered a low-top model and has a crude representation of the stratosphere, with weaker stratospheric-tropospheric coupling (Zhao et al., 2018a) compared to the atmospheric component in ESM4 (Horowitz et al., 2020). AM4.0 includes a simplified "light" chemistry model with prescribed atmospheric ozone concentrations. ESM4 employs the AM4.1 atmospheric model with 49 vertical levels extending to 1 Pa (~80 km), enhanced stratospheric vertical resolution, and comprehensive representation of atmospheric chemistry including interactive ozone (Horowitz et al., 2020). AM4.1 exhibits a better representation of the stratosphere and stratosphere-troposphere interactions (Horowitz et al., 2020). The models have different representations of sulfate aerosols that impact incident shortwave radiation (Haywood & Ramaswamy, 1998; Paulot et al., 2018), with sulfate parameterized explicitly in ESM4 and implicitly in CM4.

2.2. Experiments

Meltwater experiments are performed where a temporally uniform 0.1 Sv freshwater transport is distributed at the surface along the Antarctic coast in regions of observed ice shelf melting (Paolo et al., 2015; The IMBIE team, 2018) for 70 years under a pre-industrial control (piControl) background state. For reference, 0.1 Sv is approximately the total AIS freshwater transport expected near mid-century under Representative Concentration Pathway 8.5 (RCP8.5) determined from dynamic ice-sheet model simulations performed by DeConto and Pollard (2016). Mid-century under RCP8.5 corresponds to the approximate timing of CO_2 doubling from pre-industrial levels (see discussion in Beadling et al., 2022). It is important to note that this magnitude is on the upper end of potential mid-century AIS melt relative to other studies (Oppenheimer et al., 2019) and a 0.1 Sv

freshwater transport is large relative to observed estimates of AIS mass change (~0.004 Sv 1992 to 2017; The IMBIE team, 2018). Five ensemble members were performed for each model. Both models exhibit open-ocean polynya activity which impacts the SO climatological state on centennial timescales (Dunne, Horowitz et al., 2020; Held et al., 2019). Thus, the branch periods of the members subsample the polynya activity to reduce the response dependency on the initial SO state (see Figure A1 in Beadling et al., 2022). The meltwater enters the ocean at local SST with no latent heat fluxes accounted for. Experimental design details, including the spatial distribution of meltwater and branch points relative to polynya phasing, is found in Beadling et al. (2022), with two additional ensemble members per model completed since.

Due to the centennial-scale variability in the simulation, we average over the entire overlapping piControl period and compute differences as the last 20 years of the perturbation experiments minus the long-term piControl average (243 (CM4) and 269 (ESM4) years). This avoids potentially aliasing cyclic polynya behavior that could occur when subtracting a polynya period from a non-polynya period (or vice versa) and is consistent with Beadling et al. (2022) and Tesdal et al. (2023). Since we are analyzing the difference in the average of the last 20 years of the meltwater experiment relative to the piControl, to assess statistical significance we apply a 20 year rolling mean to the piControl fields and then compute the standard deviation to assess whether the change is outside of this measure of internal variability. All figures present stippling as values within the 90% confidence interval (CI) (<1.645 standard deviations outside of the piControl mean), that is, non-statistically significant. We present the ensemble-mean response (individual responses in Supplemental).

3. Results

3.1. Atmospheric Thermal Response

In response to AIS meltwater, both models exhibit strong near-surface (2 m) atmospheric cooling, exceeding 3°C in regions of the subpolar SO and extending, with lesser magnitudes, north of the equator (Figures 1a and 1b). Globally, this cooling amounts to an ensemble mean of ~0.4–0.5°C for CM4 and ESM4, respectively. Both models exhibit the largest surface cooling anomalies in regions where open-ocean convection is shut off via surface freshening (Chen et al., 2023), particularly within the SO Pacific sector. ESM4 exhibits more zonal uniformity in its SO surface cooling pattern owing to more meltwater entering the open SO associated with its weaker Antarctic Slope Current compared to CM4 (Beadling et al., 2022).

Temperature anomalies at 200 hPa and 50 hPa are in contrast with the surface cooling (Figures 1c–1f). We consider 200 hPa temperature changes indicative of the Upper Troposphere/Lower Stratosphere (UTLS), that is, the region of transition between the troposphere and stratosphere (Gettleman et al., 2011). The UTLS region contains the tropopause, with tropopause height diagnosed following the World Meteorological Organization (WMO, 1957) definition where tropopause height is identified as the lowest level at which the temperature lapse rate decreases to 2 K km^{-1} or less. The mean height of the tropopause varies latitudinally (Figure 2) and the SO warming at 200 hPa in the UTLS region is occurring at heights generally above the model-diagnosed tropopause (WMO defined), while the cooling farther north is generally below the tropopause. Regions of statistically significant warming are generally more broad at 200 hPa, expanding beyond the southeast Pacific as compared to the pattern of temperature increase at 50 hPa, where the warming signal is mostly confined to the subpolar Pacific over the SO (Figures 1e and 1f). The middle-to-lower stratosphere at 50 hPa is a region characterized by the presence of the polar vortex (Haynes & Shuckburgh, 2000) in the high latitude SH.

The 200 hPa pressure level is also roughly where the core of the jet streams reside, thus temperature changes at this height can influence the large-scale wind structure. The contrasting temperature response in the stratosphere and troposphere is clear in the zonal-mean temperature fields (Figures 2a and 2b). The temperature anomalies in the troposphere exhibit two distinct regions of cooling; strong cooling in the lower troposphere from the surface to the height of the tropopause south of ~30°S and a secondary region in the upper tropical troposphere between 200 and 400 hPa.

The tropopause is displaced downward, especially in regions where there is UTLS and middle-to-lower stratosphere warming (Figures 1g and 1h). To discern mechanisms behind the polar stratospheric warming, an evaluation of temperature tendency terms in the stratosphere is useful given that the leading balance for temperature tendency is between atmospheric dynamics (resolved and parameterized advective processes) and radiation. We next consider anomalies in the temperature tendency due to dynamics and the magnitude of stratospheric

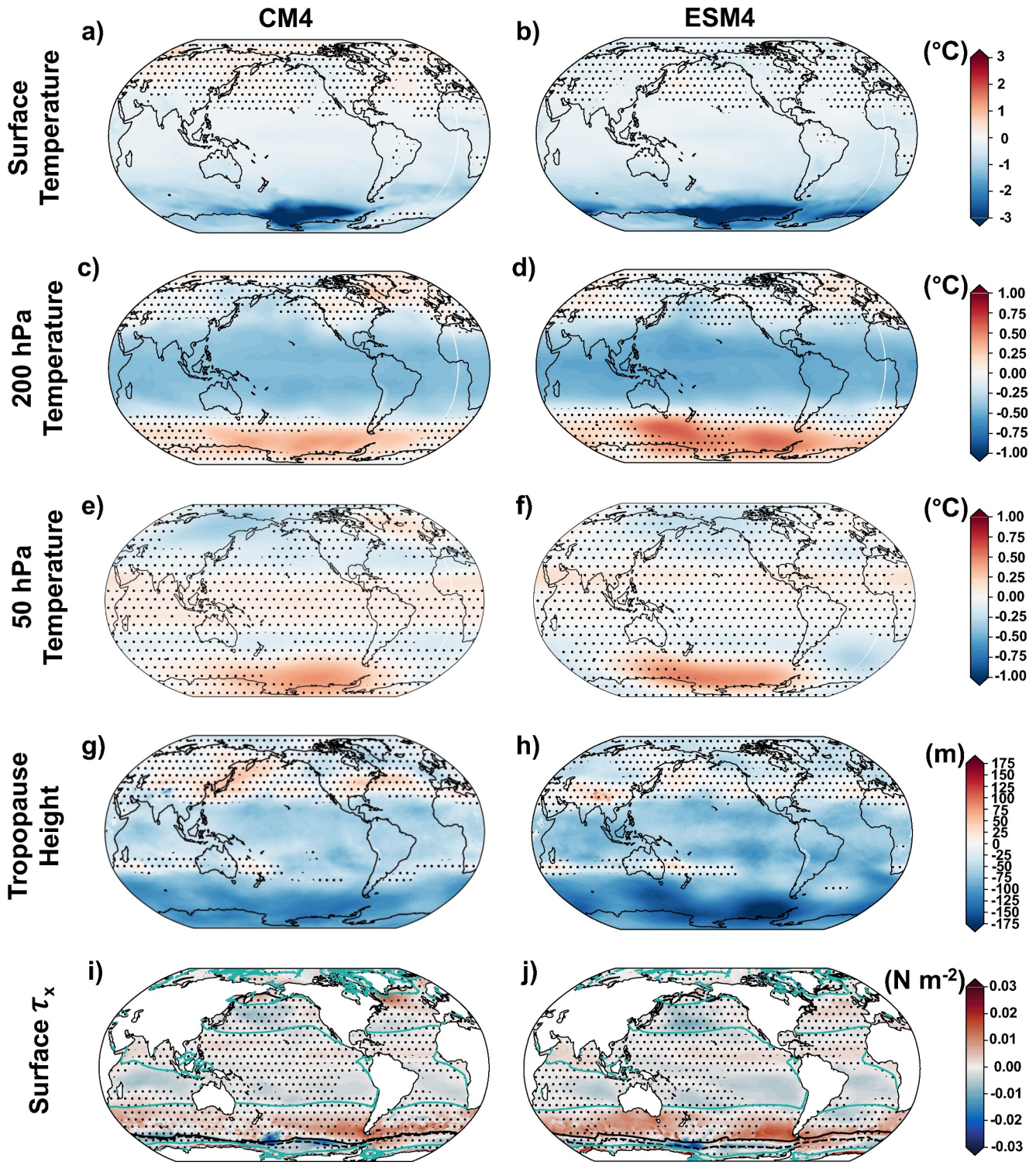

Figure 1. Ensemble-mean response of annual-mean atmospheric (a–b) near-surface, (c–d) 200 hPa, and (e–f) 50 hPa temperature (g–h) tropopause height, and (i–j) surface zonal wind stress. Stippling indicates regions that are not statistically significant at 90% CI. Teal contours in (i–j) represent the surface zero wind stress line in the long-term piControl average. Black contours in (i–j) indicate the position of the annual mean sea ice edge (where sea ice concentration is at least 15%) during the last 20 years of the experiment (solid) and piControl (dashed) long-term average.

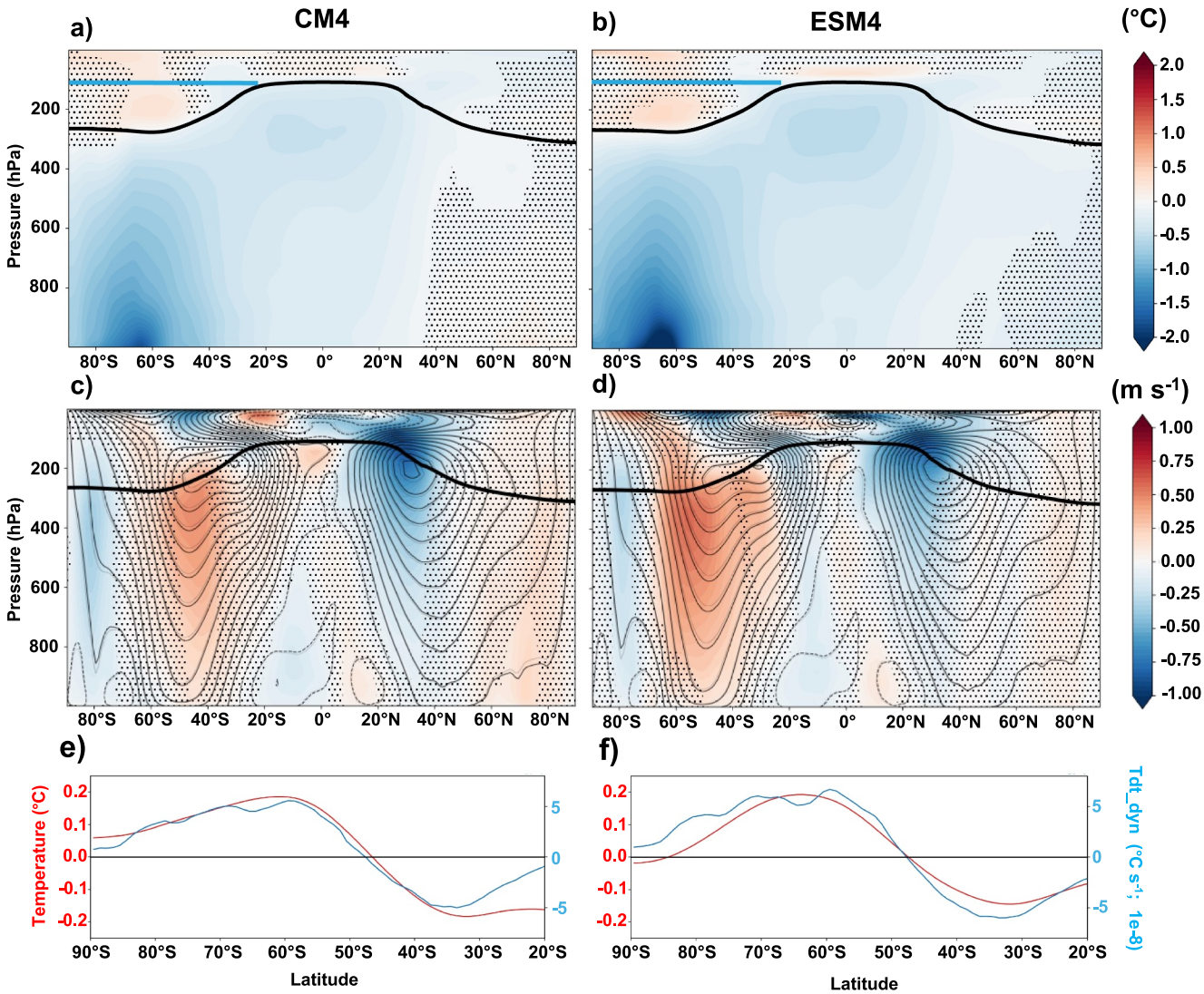

Figure 2. Ensemble mean response of annual-mean atmospheric (a–b) zonal-mean temperature, (c–d) zonal-mean zonal winds, and (e–f) 100 hPa zonal-mean temperature (red) and zonal-mean tendency of temperature due to atmospheric dynamics (blue) (blue line indicates 100 hPa in (a, b)). Stippling indicates regions that are not significant at 90% CI. The model diagnosed piControl tropopause is contoured in (a–d). In (c–d) thin contours indicate piControl zonal-mean zonal wind; thick contours indicate ensemble mean over the last 20 years of the perturbation experiment.

warming. The exact pressure levels of significant warming within the stratosphere/UTLS region differ between ensemble members (Figure S3 in Supporting Information S1), however, most exhibit warming spanning 200–10 hPa. Cross-cutting this band of warming, zonal mean temperature tendency and temperature are shown at 100 hPa (Figures 2e and 2f), however the relationship holds for higher altitudes. We find consistency between the structure of stratospheric temperature changes and the tendency due to dynamics, indicating that the temperature anomalies are occurring due to circulation change within the stratosphere potentially associated with adjustment of the Brewer-Dobson circulation, which may be affected by changes in the polar vortex as well as baroclinic instability in the troposphere.

3.2. Large-Scale Atmospheric Circulation Response

Although not statistically significant at the 90% CI throughout the full SO, both models (and all ensemble members) exhibit a distinct pattern of an intensification of surface westerly wind stress from 30°S to ~55°S and a reduction in westerly wind stress to the south of the SH sea ice edge in the subpolar SO (Figures 1i-j, Figure S1 in Supporting Information S1). While there is a distinct meridional anomaly pattern, the zonal locations of the wind

stress anomalies are not as robust across ensemble members (Figure S1 in Supporting Information S1) however the largest anomalies are in the Southeast Pacific. This sharp meridional boundary between regions of wind stress intensification and reduction corresponds to the SH sea ice edge and region of greatest surface cooling (Figures 1a and 1b), consistent with the sensible cooling effects of increased ice cover during the austral winter months. A more expansive and thicker wintertime sea ice cover inhibits sensible heat loss from the relatively warmer ocean (Figure S2 in Supporting Information S1). This, in addition to enhanced cooling via increased albedo associated with the sea ice cover, creates a sharp surface temperature gradient which influences the strength and position of surface winds in the region via thermal wind.

Anomalies in the full-column zonal winds (Figures 2c and 2d) reveal significant changes in both hemispheres and within the stratosphere and troposphere. In both models, stronger westerlies are found throughout the troposphere between 40°S and 60°S and easterly anomalies are found over Antarctica as well as in the south equatorial lower troposphere. The region of westerly wind strengthening, consistent with thermal wind balance, is co-located where there is a strong change in the meridional thermal gradient (Figures 2a and 2b) due to the strong cooling over the subpolar SO. While a relatively weak response is found in NH surface wind stress, the NH subtropical jet weakens in both models between ∼15°N and 40°N, with the largest magnitude of weakening between 500 and 100 hPa. This weakening is co-located where thermal gradients are changing due to the relatively small yet statistically significant tropical upper tropospheric cooling to the south, roughly between 400–200 hPa (Figures 2a and 2b). Within the SH polar stratosphere, zonal wind anomalies indicate a possible southward shift of the stratospheric circulation, with both models showing weaker zonal winds from 0 to 100 hPa, on the northern flank of the polar vortex. In the mid to lower troposphere over the tropics, there is an increase in the SH easterlies and a decrease in the NH which imprints on the surface wind stress noted above.

3.3. Influence on Atmospheric Composition and Radiation

Consistent with tropospheric cooling and cooler SSTs, SH column integrated water vapor content (WVP) is reduced in response to AIS meltwater (Figures 3a and 3b). The greatest magnitude of WVP decrease is found along the equator in the vicinity of the ITCZ, regions characterized in the mean state by tropical deep convection and high clouds. The same spatial patterns are found in the two models, with a slightly greater magnitude of reduction in ESM4. The increases in top of the atmosphere (TOA) outgoing longwave radiation (OLR) in the SH tropics and proximal NH OLR reduction are consistent with an ITCZ northward shift (the mean-state ITCZ is associated with an OLR minimum, thus this is associated with a movement of that minima northward). An ITCZ shift away from the colder hemisphere and into the warmer hemisphere has been documented as a response to meltwater perturbations or energy flux anomalies in previous studies (Broccoli et al., 2006; Chiang & Bitz, 2005; Kang et al., 2008; Schneider et al., 2014). There is also evidence for a slight northward ITCZ shift indicated by spatial anomalies in tropical precipitation (Figure S1 in Supporting Information S1), however these changes are subtle relative to the other responses discussed herein.

Low clouds are found primarily in regions with cold SSTs and have a net cooling effect on surface temperatures due to the reflection of incoming shortwave radiation. Both models exhibit a significant increase in SH low clouds in response to the additional meltwater consistent with previous studies (Dong et al., 2022). The greatest magnitude of increased low cloud coverage occurs over regions of strongest near-surface cooling in the subpolar South Pacific in both models. However, enhanced low cloud coverage extends further northward beyond the subpolar SO coincident with reduced SSTs (Figures 3c and 3d). Increased low cloud coverage is understood to be related to a more stable planetary boundary layer as well as a reduction in entrainment efficiency, both are associated with colder SSTs (Dong et al., 2022; Klein et al., 2017; Wood & Bretherton, 2006; Zhou et al., 2016). The spatial pattern of low cloud increase aligns with increases in TOA outgoing shortwave radiation (OSR) (Figures 3e and 3f), highlighting the contribution of low cloud coverage increase to net atmospheric cooling. The sea ice expansion and thickening in response to AIS meltwater (Beadling et al., 2022) in combination with increased low cloud coverage, enhance planetary albedo (Figure S5 in Supporting Information S1), increasing SH OSR, contributing to net atmospheric cooling (Figures 3e and 3f). A cooler surface and troposphere also reduces TOA OLR (Figures 3g and 3h).

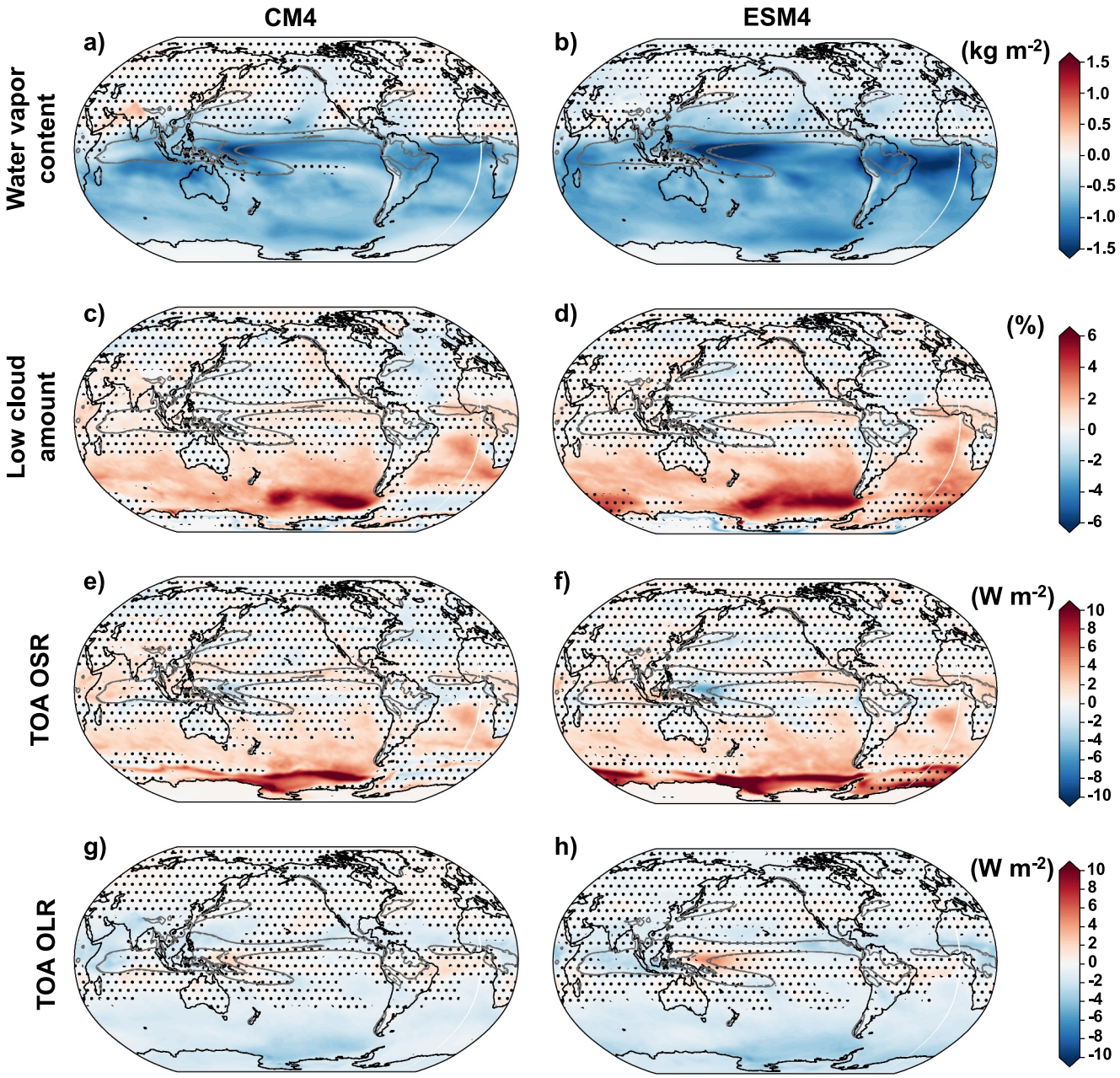

Figure 3. Ensemble mean response of annual-mean (a–b) column integrated water vapor content (WVP), (c–d) low cloud amount, (e–f) top of atmosphere (TOA) outgoing shortwave radiation (OSR), and (g–h) TOA outgoing longwave radiation (OLR). Stippling indicates regions that are not significant at 90% CI. The region of maximum annual-mean precipitation is contoured in dark gray (solid corresponding to last 20 years of experiment and dashed correspond to long-term piControl average) on each panel for perspective of changes relative to a proxy for the climatological position of the Intertropical Convergence Zone (ITCZ).

4. Discussion

We first put our results in the context of observed atmospheric changes in response to anthropogenic forcing. In response to rising atmospheric greenhouse gas (GHG) concentrations and depletion of stratospheric ozone, changes in the thermal structure and large-scale circulation of the atmosphere have been observed, including tropospheric warming and stratospheric cooling (Fu et al., 2004; Ladstädter et al., 2023; Manabe & Wetherald, 1967; Ramaswamy et al., 2001; Seidel et al., 2011; Vallis et al., 2014) and an increase in tropopause height (Santer et al., 2003a, 2003b; Lorenz & DeWeaver, 2007; Vallis et al., 2014; Meng et al., 2021). Enhanced warming in the upper tropical troposphere has been observed and is a robust modeled response to CO_2 forcing

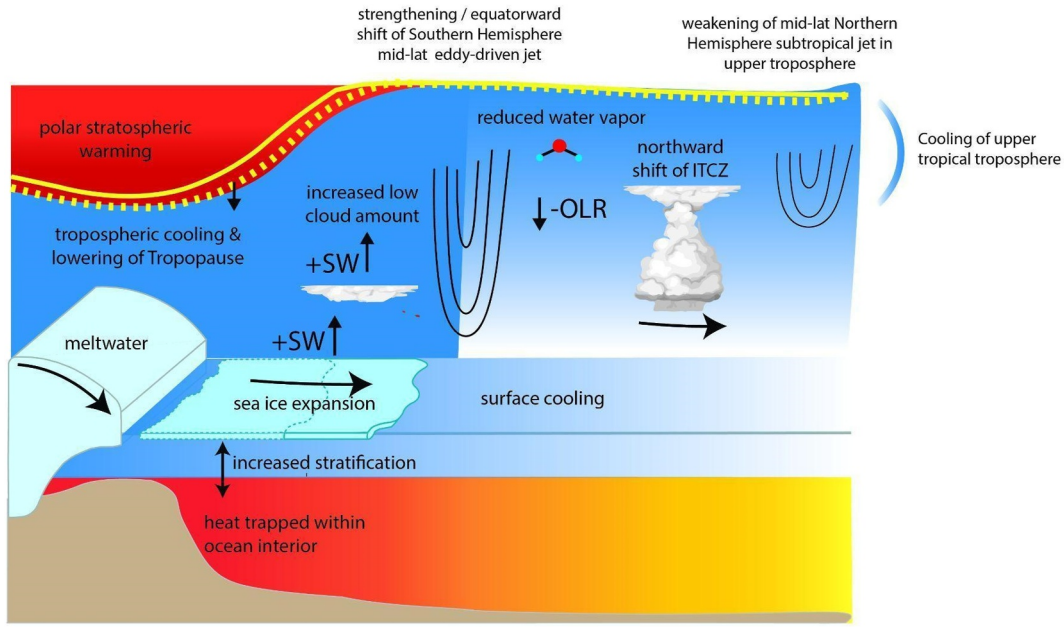

Figure 4. Schematic summarizing atmospheric dynamical and radiative response to additional meltwater in CM4 and ESM4. The + SW labels adjacent to the increased low cloud amount and sea ice expansion indicate that these processes increase top of the atmosphere (TOA) outgoing shortwave (SW) radiation and the -OLR indicates an overall decrease in TOA outgoing longwave radiation (OLR). The northward shift of the Intertropical Convergence Zone (ITCZ) is indicated by the arrow below the deep convective cloud.

(Allen & Sherwood, 2008; Ladstäder et al., 2023; Santer et al., 2005). Observed and simulated changes in global circulation patterns to anthropogenic forcing include tropical widening (Held, 1993; Seidel et al., 2008; Staten et al., 2018; Vallis et al., 2014) and a strengthening (Held, 1993; N. C. Swart and Fyfe, 2012; Vallis et al., 2014) and poleward shift of the SH eddy-driven jet (Woolings et al., 2023).

Under a pre-industrial background state, where no GHG-induced heat is added to the climate system, when meltwater is added to the surface of the Antarctic coast, our results yield responses generally opposite to the observed and modeled response to anthropogenic forcing (see 1pctCO_2 results in Supporting Information S1 for context). This "opposite-global-warming" response is brought on due to a series of positive feedbacks (Figure 4) within the climate system that can be explained by simple physical principles that govern atmospheric temperature and circulation. These feedbacks are initially set in motion by the effect of the added meltwater disrupting ocean-atmosphere heat exchange via the trapping of heat within the interior ocean due to enhanced stratification, inducing a "global-cooling effect" (Beadling et al., 2022; Bronselaer et al., 2018; Park & Latif, 2019).

As the oceanic heat inventory grows, SSTs cool and SH sea ice expands, eliciting a positive feedback resulting in further near-surface cooling through enhanced albedo. As a result of cooling SSTs, low cloud coverage increases, increasing reflected incoming shortwave (SW) radiation, contributing to further cooling of the lower and near-surface troposphere. These positive feedbacks altering planetary albedo are mostly at play in the extratropical and subpolar SH where the surface freshening is largest and sea ice expansion occurs. These are opposite to what occurs in a climate that is warming in response to GHG forcing, whereby planetary albedo decreases with high-latitude sea ice loss (Manabe & Stouffer, 1979) and reduced low cloud coverage, increasing surface SW absorption (Held, 1993). In addition to shortwave cooling, the reduced WVP of a cooler troposphere decreases the amount of longwave (LW) absorbed given its role as a GHG. Atmospheric moisture content plays a particularly important role in the tropical troposphere, where the vertical profile of atmospheric temperature approximates a moist adiabat (Fu et al., 2004; Manabe & Wetherald, 1967; Stone & Carlson, 1979) and thus changes in tropical surface temperatures are amplified in the upper-tropical troposphere. The weaker surface cooling of ~0.25°C simulated in the tropics in both models is amplified to ~0.40°C in the upper troposphere. This result is an important example of how Antarctic meltwater can have remote effects on the global atmosphere structure, connecting to the upper tropical troposphere.

Another far-reaching impact that our results highlight is a robust warming of the mid to lower stratosphere in the SH and a coinciding downward displacement of the tropopause. Our results suggest that this SH stratospheric warming is aligned primarily with changes in advective processes within the stratosphere, which may be a result of the downward tropopause displacement itself. However, disentangling the details of the mechanisms driving stratospheric warming requires additional higher frequency model output and further analysis. The fact that both models produce very similar stratospheric temperature responses, while ESM4 includes interactive ozone chemistry and CM4 prescribes ozone, also suggests that these warming patterns are primarily a result of changing physical circulation rather than a radiative response. A downward displacement of the tropopause has implications for large-scale circulation given the role of tropopause height as an important dynamical scale for atmospheric waves and circulation. Previous studies reported a more equatorward stormtrack resulting from a lower tropopause (Lorenz & DeWeaver, 2007; Williams, 2006).

As a result of changes in the vertical and horizontal temperature gradients, the global large-scale circulation is altered in both models. A strengthening of the eddy-driven SH jet is aligned with an increasing meridional temperature gradient due to strong surface cooling in the middle to lower troposphere over the SO (Broccoli et al., 2006). A robust meridional shift of the SH eddy-driven jet is less apparent in our results. Interestingly, the strengthening of the eddy-driven SH jet is the only response that is not opposite to the climate response to GHG forcing, with a strengthening of this jet expected under increased anthropogenic forcing (Held, 1993; N. C. Swart and Fyfe, 2012; Vallis et al., 2014). The pattern of increase in the SH zonal mean winds in response to the meltwater perturbation in this study is qualitatively similar to that which occurs near the time of CO_2 doubling in 1pctCO_2 simulations in these same models (Figure S8 in Supporting Information S1), but of lesser magnitude (strengthening ∼25% weaker in meltwater simulations analyzed here).

There are also significant changes in the NH subtropical jet near the tropopause. Unlike the SH eddy-driven jet response discussed above, the NH subtropical jet response appears to be opposite to that expected in a 1pctCO_2 simulation (Figure S8 in Supporting Information S1). The magnitude of the changes in the NH subtropical jet are surprising given the relatively small (but statistically significant and robust) changes in the upper troposphere and lower stratosphere temperature in the NH. Understanding the dynamics governing this weakening of the NH subtropical jet deserves a detailed follow-on study as there might be more mechanisms at play beyond simple thermal wind balance.

While the existing literature on the full atmospheric response to AIS meltwater is sparse, several studies have imposed asymmetric anomalies in surface energy fluxes or high-latitude sea ice. These studies support our results that high-latitude anomalies can impart deep-reaching effects on the tropics, upper atmosphere, and jet stream dynamics (Broccoli et al., 2006; Chiang & Bitz, 2005; England et al., 2018, 2020a; Kang et al., 2008; Kidston et al., 2011; Screen et al., 2018; Smith et al., 2022). The pronounced asymmetric WVP reduction limited to the SH, is consistent with Chiang and Bitz (2005), which imposed a positive sea ice extent anomaly in a slab-ocean configuration and investigated ITCZ displacement. Chiang and Bitz (2005) suggest that the reduced atmospheric moisture is important in propagating the cold SST anomalies toward the equator followed by an anomalous circulation that causes the cold, dry hemisphere to "feed moisture" across the equator resulting in a sharp moisture gradient near the ITCZ. The sharp WVP gradient (Figures 3a and 3b) and anomalies in latent heat transport simulated by CM4 and ESM4 support this mechanism (Figure S6 in Supporting Information S1). Chiang and Bitz (2005) also show strong tropospheric cooling coinciding with stratospheric warming in the cold dry hemisphere (NH in their case), mirroring our results in the SH, however, there is no discussion of mechanisms driving the stratospheric warming. Our full column zonal mean temperature response is directly opposite to the response found by England, Wagner, and Eisenman (2020) in experiments where SH sea ice is reduced (in the experiments here sea ice expands due to meltwater forcing). Our changes in the SH wind stress and jet stream are also consistent with that from Kidston et al. (2011) which imposed a SH sea ice expansion anomaly.

5. Conclusions

Our results underscore the global influence of AIS melting, highlighting that climate impacts not only extend from the surface through the abyssal ocean but also throughout the global troposphere to the stratosphere. In the piControl simulations considered here, with no GHG-induced warming, the global atmospheric response is generally opposite to what has been observed or simulated in response to anthropogenic forcing. Tropospheric cooling extending from the surface to the tropopause is the result of a series of positive feedbacks working to

increase planetary albedo and reduce atmospheric water vapor content. This "opposite-global-warming" thermal response in the troposphere can be understood through fundamental principles that govern the vertical profile of the troposphere such as the moist adiabatic lapse rate propagating cooling anomalies into the upper tropical troposphere. While observed cooling in the stratosphere is mainly contributed by the radiative effect of ozone depletion and GHG increase, our analysis indicates that the simulated stratospheric warming in response to AIS meltwater is linked to the changing circulation within the stratosphere, that is, there are very different mechanisms at play. Understanding the details of how the stratospheric circulation responds to tropospheric cooling warrants further study.

Changes in the thermal structure of the atmosphere as a result of the meltwater forcing impact the jet streams in both hemispheres, highlighting the potential for disruption of mid-latitude climate patterns. Contrasting with the rest of the responses discussed here, the strengthening response of the SH eddy-driven jet to AIS meltwater is in agreement with changes expected under increased GHG warming. We can qualitatively compare the results presented here to those documented in GHG warming simulations to provide context, however, our experiments were performed in a pre-industrial background state, limiting our understanding of how these coupled dynamics will play out in a warming climate. While the global cooling anomalies found here are well below the magnitude of global warming realized and expected by the end of the 21st century (Gulev et al., 2021), it remains unknown whether the changes in atmospheric dynamics due to AIS melting found here may partially compensate GHG-driven changes. Applying these perturbations in a future climate scenario is planned for future study.

While we have found robust agreement in the two climate models used here, it remains unclear whether these results will hold across other simulations, particularly concerning stratospheric warming. There are important differences in the atmospheric components and the ocean model formulations of CM4 and ESM4, however, both models exhibit strong open-ocean convection in the subpolar SO in their mean-state. Production of dense water via open-ocean convection, in the form of polynyas in the Weddell and Ross Seas, as opposed to realistic formation via dense shelf water (DSW) is a long-standing bias that many coupled climate models continue to suffer from (Heuzé, 2021; Heuzé et al., 2013). Despite more coastal processes being resolved in the 0.25° CM4 configuration and more realistic DSW production, even higher resolution is needed to fully resolve dense water formation processes on the shelf. As a result, the interplay between open-ocean convection, surface temperatures, and sea ice may complicate the interpretation of our results and should motivate repeating our experimental design in higher-resolution models. The spatial details and the magnitude of the response shown here may differ in models with differing degrees of SO stability and more realistic dense water formation mechanisms.

The meltwater perturbations in the experiments presented here were idealized in the sense that they were imposed at the ocean surface, at local SST, and with no seasonal variation in the magnitude of the freshwater fluxes. There may be differing responses with more realistic subsurface freshwater delivery and delivery via icebergs (England, Polvani, et al., 2020), the inclusion of latent heat extraction required for melting ice, and seasonal variations. To address the uncertainties associated with the caveats listed herein, additional simulations must be performed under more realistic climate scenarios and with the inclusion of dynamic ice sheet components. An investigation of model dependence and sensitivity of the climate response to methods of meltwater perturbation implementation is planned as part of the Southern Ocean Freshwater Input from Antarctica (SOFIA) Initiative (Swart et al., 2023).

Data Availability Statement

The freshwater forcing fields used in these experiments are available via Zenodo (R. Beadling, 2024a). The piControl and 1pctCO_2 CM4 (Guo et al., 2018a, 2018b) and ESM4 (Krasting et al., 2018a, 2018b) model output is archived and available for download at the Earth System Grid Federation (https://esgf.llnl.gov/). Model output for the experiments presented here and associated analysis code is available via Zenodo for CM4 (R. Beadling, 2024b) and ESM4 (R. Beadling, 2024c). Analysis and production of figures in this manuscript utilized Matplotlib version 3.5.1 (Hunter, 2007) available under Matplotlib license at https://matplotlib.org/, Xarray version 2022.3.0 (Hoyer & Hamman, 2017) available under Xarray license at https://docs.xarray.dev/, Cartopy version 0.20.2 available under Cartopy license at https://scitools.org.uk/cartopy/, and momlevel version 0.0.6 available at https://momlevel.readthedocs.io/en/v0.0.11/.

Acknowledgments
RLB was supported under NSF Division of Polar Programs Grant NSF2319828. This report was prepared by PL under award NA18OAR4320123 from NOAA, U.S. Department of Commerce. The statements, findings, conclusions, and recommendations are those of the author(s) and do not necessarily reflect the views of NOAA, or the U.S. Department of Commerce. MJM was supported by the U.S. DOE, Office of Science DE-SC0022070 and NSF IA 1947282, and by the NCAR, which is sponsored by the NSF. The authors thank Nadir Jeevanjee, Ronald J. Stouffer, Molly Menzel, the editor, and two anonymous reviewers for comments that greatly improved the manuscript.

References

Adcroft, A., Anderson, W., Balaji, V., Blanton, C., Bushuk, M., Dufour, C. O., et al. (2019). The GFDL global ocean and sea ice model OM4.0: Model description and simulation features. *Journal of Advances in Modeling Earth Systems*, *11*(10), 3167–3211. https://doi.org/10.1029/2019ms001726

Allen, R. J., & Sherwood, S. (2008). Warming maximum in the tropical upper troposphere deduced from thermal winds. *Nature*, *1*(6), 399–403. https://doi.org/10.1038/ngeo208

Beadling, R. (2024a). Beadling_2022_JGROceans. *Zenodo*. [Dataset]. https://doi.org/10.5281/zenodo.11149460

Beadling, R. (2024b). beadling_gfdl_cm4_submission. *Zenodo*. [Dataset]. https://doi.org/10.5281/zenodo.11182977

Beadling, R. (2024c). beadling_gfdl_esm4_submission. *Zenodo*. [Dataset]. https://doi.org/10.5281/zenodo.11222155

Beadling, R. L., Krasting, J. P., Griffies, S. M., Hurlin, W. J., Bronselaer, B., Russell, J. L., et al. (2022). Importance of the Antarctic Slope Current in the Southern Ocean response to ice sheet melt and wind stress change. *Journal of Geophysical Research: Oceans*, *127*(5), e2021JC017608. https://doi.org/10.1029/2021jc017608

Broccoli, A. J., Dahl, K. A., & Stouffer, R. J. (2006). Response of the ITCZ to northern hemisphere cooling. *Geophysical Research Letters*, *33*(1), L01702. https://doi.org/10.1029/2005gl024546

Bronselaer, B., Winton, M., Griffies, S. M., Hurlin, W. J., Rodgers, K. B., Sergienko, O. V., et al. (2018). Change in future climate due to Antarctic meltwater. *Nature*, *564*(7734), 53–58. https://doi.org/10.1038/s41586-018-0712-z

Chen, J.-J., Swart, N. C., Beadling, R., Cheng, X., Hattermann, T., Jüling, A., et al. (2023). Reduced deep convection and bottom water formation due to Antarctic meltwater in a multi-model ensemble. *Geophysical Research Letters*, *50*(24), e2023GL106492. https://doi.org/10.1029/2023gl106492

Chiang, J. C. H., & Bitz, C. M. (2005). Influence of high latitude ice cover on the marine Intertropical Convergence Zone. *Climate Dynamics*, *25*(5), 477–496. https://doi.org/10.1007/s00382-005-0040-5

DeConto, R. M., & Pollard, D. (2016). Contribution of Antarctica to past and future sea-level rise. *Nature*, *531*(7596), 591–597. https://doi.org/10.1038/nature17145

Dong, Y., Pauling, A. G., Sadai, S., & Armour, K. (2022). Antarctic ice-sheet meltwater reduces transient warming and climate sensitivity through the sea-surface temperature pattern effect. *Geophysical Research Letters*, *49*(24), e2022GL101249. https://doi.org/10.1029/2022gl101249

Dunne, J. P., Bociu, I., Bronselaer, B., Guo, H., John, J. G., Krasting, J. P., et al. (2020a). Simple global ocean Biogeochemistry with Light, Iron, Nutrients and Gas version 2 (BLINGv2): Model description and simulation characteristics in GFDL's CM4.0. *Journal of Advances in Modeling Earth Systems*, *12*(10), e2019MS002008. https://doi.org/10.1029/2019ms002008

Dunne, J. P., Horowitz, L. W., Adcroft, A. J., Ginoux, P., Held, I. M., John, J. G., et al. (2020b). The GFDL Earth System Model Version 4.1 (GFDL-ESM 4.1): Overall coupled model description and simulation characteristics. *Journal of Advances in Modeling Earth Systems*, *12*(11), e2019MS002015. https://doi.org/10.1029/2019ms002015

England, M., Polvani, L., & Sun, L. (2018). Contrasting the Antarctic and Arctic atmospheric responses to projected sea ice loss in the late twenty-first century. *Journal of Climate*, *31*(16), 6353–6370. https://doi.org/10.1175/jcli-d-17-0666.1

England, M. R., Polvani, L. M., Sun, L., & Deser, C. (2020). Tropical climate responses to projected Arctic and Antarctic sea-ice loss. *Nature Geoscience*, *13*(4), 275–281. https://doi.org/10.1038/s41561-020-0546-9

England, M. R., Wagner, T. J. W., & Eisenman, I. (2020). Modeling the breakup of tabular icebergs. *Science Advances*, *6*(51), eabd1273. https://doi.org/10.1126/sciadv.abd1273

Fox-Kemper, B., Hewitt, H. T., Xiao, C., Aðalgeirsdóttir, G., Drijfhout, S. S., Edwards, T. L., et al. (2021). Ocean, cryosphere, and sea level change, in: Climate change 2021: The physical science basis. In V. Masson-Delmotte, P. Zhai, A. Pirani, S. L. Connors, C. Péan, S. Berger, et al. (Eds.), *Contribution of working group I to the sixth assessment report of the intergovernmental panel on climate change* (pp. 1211–1362). Cambridge University Press. https://doi.org/10.1017/9781009157896.001

Fu, Q., Johanson, C. M., Warren, S. G., & Seidel, D. J. (2004). Contribution of stratospheric cooling to satellite-inferred tropospheric temperature trends. *Nature*, *429*(6987), 55–58. https://doi.org/10.1038/nature02524

Gettelman, A., Hoor, P., Pan, L. L., Randel, W. J., Hegglin, M. I., & Birner, T. (2011). The extratropical upper troposphere and lower stratosphere. *Reviews of Geophysics*, *49*(3), RG3003. https://doi.org/10.1029/2011rg000355

Gulev, S. K., Thorne, P. W., Ahn, J., Dentener, F. J., Domingues, C. M., Gerland, S., et al. (2021). Changing state of the climate system. In climate change 2021: The physical science basis. In V. P. Zhai, A. Pirani, S. L. Connors, C. Péan, S. Berger, N. Caud, et al. (Eds.), *Contribution of working group I to the sixth assessment report of the intergovernmental panel on climate change [Masson-Delmotte* (pp. 287–422). Cambridge University Press.

Guo, H., & Coauthors (2018a). NOAA-GFDL GFDL-CM4 model output piControl. *Earth System Grid Federation*. [Dataset]. https://doi.org/10.22033/ESGF/CMIP6.8666

Guo, H., & Coauthors (2018b). NOAA-GFDL GFDL-CM4 model output 1pctCO2. *Earth System Grid Federation*. [Dataset]. https://doi.org/10.22033/ESGF/CMIP6.8470

Haynes, P., & Shuckburgh, E. (2000). Effective diffusivity as a diagnostic of atmospheric transport: 2. Troposphere and lower stratosphere. *Journal of Geophysical Research*, *105*(D18), 22795–22810. https://doi.org/10.1029/2000jd900092

Haywood, J. M., & Ramaswamy, V. (1998). Global sensitivity studies of the direct radiative forcing due to anthropogenic sulfate and black carbon aerosols. *Journal of Geophysical Research*, *103*(D6), 6043–6058. https://doi.org/10.1029/97jd03426

Held, I. M. (1993). Large-scale dynamics and global warming. *Bulletin of the American Meteorological Society*, *74*(2), 228–241. https://doi.org/10.1175/1520-0477(1993)074<0228:lsdagw>2.0.co;2

Held, I. M., & Coauthors (2019). Structure and performance of GFDL's CM4.0 climate model. *Journal of Advances in Modeling Earth Systems*, *11*, 3691–3727. https://doi.org/10.1029/2019MS001829

Held, I. M., & Soden, B. J. (2006). Robust responses of the hydrological cycle to global warming. *Journal of Climate*, *19*(21), 5686–5699. https://doi.org/10.1175/jcli3990.1

Heuzé, C. (2021). Antarctic bottom water and north atlantic deep water in CMIP6 models. *Ocean Science*, *17*(1), 59–90. https://doi.org/10.5194/os-17-59-2021

Heuzé, C., Heywood, K., Stevens, D., & Ridley, J. (2013). Southern Ocean bottom water characteristics in CMIP5 models. *Geophysical Research Letters*, *40*(7), 1409–1414. https://doi.org/10.1002/grl.50287

Horowitz, L. W., Naik, V., Paulot, F., Ginoux, P. A., Dunne, J. P., Mao, J., et al. (2020). The GFDL global atmospheric chemistry-climate model AM4.1: Model description and simulation characteristics. *Journal of Advances in Modeling Earth Systems*, *12*(10), e2019MS002032. https://doi.org/10.1029/2019ms002032

Hoyer, S., & Hamman, J. (2017). xarray: N-D labeled Arrays and Datasets in Python. *Journal of Open Research Software*, *5*(1), 10. https://doi.org/10.5334/jors.148

Hunter, J. D. (2007). Matplotlib: A 2d graphics environment. *Computing in Science and Engineering*, *9*(3), 90–95. https://doi.org/10.1109/MCSE.2007.55

IMBIE team, T. (2018). Mass balance of the antarctic ice sheet from 1992 to 2017. *Nature*, *558*(7709), 219–222. https://doi.org/10.1038/s41586-018-0179-y

Kang, M. S., Held, I. M., F Dargan, M. W., & Zhao, M. (2008). The response of the ITCZ to extratropical thermal forcing: Idealized slab-ocean experiments with a GCM. *Journal of Climate*, *21*(14), 3521–3532. https://doi.org/10.1175/2007jcli2146.1

Kidston, J., Taschetto, A., Tompson, D., & England, M. (2011). The influence of Southern Hemisphere sea ice extent on the latitude of the mid-latitude jet stream. *Geophysical Research Letters*, *38*(15), L15804. https://doi.org/10.1029/2011gl048056

Klein, S. A., Hall, A., Norris, J. R., & Pincus, R. (2017). Low-cloud feedbacks from cloud-controlling factors: A review. In R. Pincus, D. Winker, S. Bony, & B. Stevens (Eds.), *Shallow clouds, water vapor, circulation, and climate sensitivity. Space sciences series of ISSI* (p. 65). Springer.

Krasting, J. P., & Coauthors (2018a). NOAA-GFDL GFDL-ESM4 model output prepared for CMIP6 CMIP piControl. *Earth System Grid Federation*. [Dataset]. https://doi.org/10.22033/ESGF/CMIP6.8669

Krasting, J. P., & Coauthors (2018b). NOAA-GFDL GFDL-ESM4 model output prepared for CMIP6 CMIP 1pctCO2. *Earth System Grid Federation*. [Dataset]. https://doi.org/10.22033/ESGF/CMIP6.8473

Ladstäder, F., Steiner, A. K., & Gleisner, H. (2023). Resolving the 21st century temperature trends of the upper troposphere-lower stratosphere with satellite observations. *Scientific Reports*, *13*(1), 1306. https://doi.org/10.1038/s41598-023-28222-x

Lorenz, D. J., & DeWeaver, E. T. (2007). Tropopause height and zonal wind response to global warming in the IPCC scenario integrations. *Journal of Geophysical Research*, *112*(D10), D10119. https://doi.org/10.1029/2006jd008087

Ma, H., & Wu, L. (2011). Global teleconnections in response to freshening over the Antarctic ocean. *Journal of Climate*, *24*(4), 1071–1088. https://doi.org/10.1175/2010jcli3634.1

Manabe, S., & Stouffer, R. (1979). CO2-climate sensitivity study with a mathematical model of the global climate. *Nature*, *282*(5738), 491–493. https://doi.org/10.1038/282491a0

Manabe, S., & Wetherald, R. T. (1967). Thermal equilibrium of the atmosphere with a given distribution of relative humidity. *Journal of the Atmospheric Sciences*, *24*(3), 241–259. https://doi.org/10.1175/1520-0469(1967)024<0241:teotaw>2.0.co;2

Meng, L., Liu, J., Tarasick, D. W., Randel, W. J., Steiner, A. K., Wilhelmsen, H., et al. (2021). Continuous rise of the tropopause in the northern hemisphere over 1980–2020. *Science Advances*, *7*(45), eabi8065. https://doi.org/10.1126/sciadv.abi8065

Oppenheimer, M., Glavovic, B. C., Hinkel, J., van de Wal, R., Magnan, A. K., Abd-Elgawad, A., et al. (2019). Sea level rise and implications for low-lying islands, coasts and communities. In D. C. Roberts, V. Masson-Delmotte, P. Zhai, M. Tignor, E. Poloczanska, K. Mintenbeck, et al. (Eds.), *IPCC special report on the ocean and cryosphere in a changing climate [H.-O. Pörtner]*.

Paolo, F. S., Fricker, H. A., & Padman, L. (2015). Volume loss from Antarctic ice shelves is accelerating. *Science*, *348*(6232), 327–331. https://doi.org/10.1126/science.aaa0940

Park, W., & Latif, M. (2019). Ensemble global warming simulations with idealized Antarctic meltwater input. *Climate Dynamics*, *52*(5–6), 3223–3239. https://doi.org/10.1007/s00382-018-4319-8

Paulot, F., Paynter, D., Ginoux, P., Naik, V., & Horowitz, L. W. (2018). Changes in the aerosol direct radiative forcing from 2001 to 2015: Observational constraints and regional mechanisms. *Atmospheric Chemistry and Physics*, *18*(17), 13265–13281. https://doi.org/10.5194/acp-18-13265-2018

Ramaswamy, V., & Coauthors (2001). Stratospheric temperature trends: Observations and model simulations. *Reviews of Geophysics*, *39*, 12–71.

Santer, B. D., Sausen, R., Wigley, T. M. L., Boyle, J. S., AchutaRao, K., Doutriaux, C., et al. (2003). Behavior of tropopause height and atmospheric temperature in models, reanalyses, and observations: Decadal changes. *Journal of Geophysical Research*, *108*(D1), 4002. https://doi.org/10.1029/2002jd002258

Santer, B. D., Wehner, M. F., Wigley, T. M. L., Sausen, R., Meehl, G. A., Taylor, K. E., et al. (2003). Contributions of anthropogenic and natural forcing to recent tropopause height changes. *Science*, *301*(5632), 479–483. https://doi.org/10.1126/science.1084123

Santer, B. D., Wigley, T. M. L., Mears, C., Wentz, F. J., Klein, S. A., Seidel, D. J., et al. (2005). Amplification of surface temperature trends and variability in the tropical atmosphere. *Science*, *309*(5740), 1551–1556. https://doi.org/10.1126/science.1114867

Schmidt, G. A., Romanou, A., Roach, L., Mankoff, K., Li, Q., Rye, C. D., et al. (2023). Anomalous meltwater from ice sheets and ice shelves is a historical forcing. *Geophysical Research Letters*, *50*(24), e2023GL106530. https://doi.org/10.1029/2023gl106530

Schneider, T., Bischoff, T., & Haug, G. (2014). Migrations and dynamics of the intertropical convergence zone. *Nature*, *513*(7516), 45–53. https://doi.org/10.1038/nature13636

Screen, J. A., Deser, C., Smith, D. M., Zhang, X., Blackport, R., Kushner, P. J., et al. (2018). Consistency and discrepancy in the atmospheric response to Arctic sea-ice loss across climate models. *Nature Geoscience*, *11*(3), 155–163. https://doi.org/10.1038/s41561-018-0059-y

Seidel, D. J., Fu, Q., Randel, W. J., & Reichler, T. J. (2008). Widening of the tropical belt in a changing climate. *Nature Geoscience*, *1*, 21–24. https://doi.org/10.1038/ngeo.2007.38

Seidel, D. J., Gillett, N. P., Lanzante, J. R., Shine, K. P., & Thorne, P. W. (2011). Stratospheric temperature trends: Our evolving understanding. *WIREs Climate Change*, *2*(4), 592–616. https://doi.org/10.1002/wcc.125

Smith, B., Fricker, H. A., Gardner, A. S., Medley, B., Nilsson, J., Paolo, F. S., et al. (2020). Pervasive ice sheet mass loss reflects competing ocean and atmosphere processes. *Science*, *368*(6496), 1239–1242. https://doi.org/10.1126/science.aaz5845

Smith, D. M., Eade, R., Andrews, M. B., Ayres, H., Clark, A., Chripko, S., et al. (2022). Robust but weak winter atmospheric circulation response to future Arctic sea ice loss. *Nature Communications*, *13*(1), 727. https://doi.org/10.1038/s41467-022-28283-y

Staten, P. W., Lu, J., Grise, K. M., Davis, S. M., & Birner, T. (2018). Re-examining tropical expansion. *Nature Climate Change*, *8*(9), 768–775. https://doi.org/10.1038/s41558-018-0246-2

Stone, P. H., & Carlson, J. H. (1979). Atmospheric lapse rate regimes and their parameterization. *Journal of the Atmospheric Sciences*, *36*(3), 415–423. https://doi.org/10.1175/1520-0469(1979)036<0415:alrrat>2.0.co;2

Stouffer, R. J., Seidov, D., & Haupt, B. J. (2007). Climate response to external sources of freshwater: North atlantic versus the Southern Ocean. *Journal of Climate*, *20*(3), 436–448. https://doi.org/10.1175/jcli4015.1

Swart, N. C., & Coauthors (2023). The Southern Ocean Freshwater input from Antarctica (SOFIA) initiative: Scientific objectives and experimental design. *Geoscience Model Development*, *16*, 7289–7309.

Swart, N. C., & Fyfe, J. C. (2012). Observed and simulated changes in the Southern Hemisphere surface westerly wind-stress. *Geophysical Research Letters*, *39*(16), L16711. https://doi.org/10.1029/2012gl052810

Tesdal, J.-E., MacGilchrist, G. A., Beadling, R. L., Griffies, S. M., Krasting, J. P., & Durack, P. J. (2023). Revisiting interior water mass responses to surface forcing changes and the subsequent effects on overturning in the Southern Ocean. *Journal of Geophysical Research: Oceans*, *128*(3), e2022JC019105. https://doi.org/10.1029/2022jc019105

Vallis, G. K., Zurita-Gotor, P., Cairns, C., & Kidston, J. (2014). Response of the large-scale structure of the atmosphere to global warming. *Quarterly Journal of the Royal Meteorological Society*, *141*(690), 1479–1501. https://doi.org/10.1002/qj.2456

Williams, G. P. (2006). Circulation sensitivity to tropopause height. *Journal of the Atmospheric Sciences*, *63*(7), 1954–1961. https://doi.org/10.1175/jas3762.1

Wood, R., & Bretherton, C. S. (2006). On the relationship between stratiform low cloud cover and 181 lower-tropospheric stability. *Journal of Climate*, *19*(24), 6425–6432. https://doi.org/10.1175/jcli3988.1

Woollings, T., Drouard, M., O'Reilly, C. H., Sexton, D. M. H., & McSweeny, C. (2023). Trends in the atmospheric jet streams are emerging in observations and could be linked to tropical warming. *Communication Earth Environment*, *4*(1), 125. https://doi.org/10.1038/s43247-023-00792-8

World Meteorological Organization (WMO). (1957). Definition of the tropopause. *World Meteorological Organization Bulletin*, *6*, 136.

Zhao, M., & Coauthors (2018a). The GFDL global atmosphere and land model AM4. 0/LM4. 0: 1. Simulation characteristics with prescribed SSTs. *Journal of Advances in Modeling Earth Systems*, *10*, 735–769. https://doi.org/10.1002/2017MS001208

Zhao, M., & Coauthors (2018b). The GFDL global atmosphere and land model AM4. 0/LM4.1360 0: 2. Model description, sensitivity studies, and tuning strategies. *Journal of Advances in Modeling Earth Systems*, *10*, 691–734. https://doi.org/10.1002/2017MS001209

Zhou, C., Zelinka, M., & Klein, S. (2016). Impact of decadal cloud variations on the Earth's energy budget. *Nature Geoscience*, *9*(12), 871–874. https://doi.org/10.1038/ngeo2828